mathematics

MDPI

Article

Fatigue Estimation Using Peak Features from PPG Signals

Yi-Xiang Chen [1], Chin-Kun Tseng [2,3], Jung-Tsung Kuo [2], Chien-Jen Wang [2,4], Shu-Hung Chao [2], Lih-Jen Kau [2], Yuh-Shyan Hwang [2] and Chun-Ling Lin [1,*]

1 Department of Electrical Engineering, Ming Chi University of Technology, No. 84, Gongzhuan Rd., Taishan Dist., New Taipei City 243, Taiwan; ivan81030@gmail.com
2 Department of Electronic Engineering, National Taipei University of Technology, Taipei 106, Taiwan; richardtseng2@yahoo.com.tw (C.-K.T.); a0911779983@gmail.com (J.-T.K.); master.jr.wang@gmail.com (C.-J.W.); chao.suhon@gmail.com (S.-H.C.); ljkau@ntut.edu.tw (L.-J.K.); yshwang@ntut.edu.tw (Y.-S.H.)
3 Division of Cardiology, Tri-Service General Hospital, Songshan Branch, Taipei 105, Taiwan
4 Center for Traditional Medicine, Taipei Veterans General Hospital, Taipei 112, Taiwan
* Correspondence: ginnylin@mail.mcut.edu.tw

Abstract: Fatigue is a prevalent subjective sensation, affecting both office workers and a significant global population. In Taiwan alone, over 2.6 million individuals—around 30% of office workers—experience chronic fatigue. However, fatigue transcends workplaces, impacting people worldwide and potentially leading to health issues and accidents. Gaining insight into one's fatigue status over time empowers effective management and risk reduction associated with other ailments. Utilizing photoplethysmography (PPG) signals brings advantages due to their easy acquisition and physiological insights. This study crafts a specialized preprocessing and peak detection methodology for PPG signals. A novel fatigue index stems from PPG signals, focusing on the dicrotic peak's position. This index replaces subjective data from the brief fatigue index (BFI)-Taiwan questionnaire and heart rate variability (HRV) indices derived from PPG signals for assessing fatigue levels. Correlation analysis, involving sixteen healthy adults, highlights a robust correlation ($R > 0.53$) between the new fatigue index and specific BFI questions, gauging subjective fatigue over the last 24 h. Drawing from these insights, the study computes an average of the identified questions to formulate the evaluated fatigue score, utilizing the newfound fatigue index. The implementation of linear regression establishes a robust fatigue assessment system. The results reveal an impressive 91% correlation coefficient between projected fatigue levels and subjective fatigue experiences. This underscores the remarkable accuracy of the proposed fatigue prediction in evaluating subjective fatigue. This study further operationalized the proposed PPG processing, peak detection method, and fatigue index using C# in a computer environment alongside a PPG device, thereby offering real-time fatigue indices to users. Timely reminders are employed to prompt users to take notice when their index exceeds a predefined threshold, fostering greater attention to their physical well-being.

Keywords: fatigue; photoplethysmography (PPG); heart rate variability (HRV); brief fatigue index (BFI)-Taiwan form

MSC: 62P10; 68T09

check for updates

Citation: Chen, Y.-X.; Tseng, C.-K.; Kuo, J.-T.; Wang, C.-J.; Chao, S.-H.; Kau, L.-J.; Hwang, Y.-S.; Lin, C.-L. Fatigue Estimation Using Peak Features from PPG Signals. *Mathematics* **2023**, *11*, 3580. https://doi.org/10.3390/math11163580

Academic Editors: Jordi Martorell-Marugán and Pedro Carmona-Sáez

Received: 31 July 2023
Revised: 14 August 2023
Accepted: 16 August 2023
Published: 18 August 2023

1. Introduction

"Fatigue" is a subjective feeling that everyone experiences. Fatigue slows down the brain's ability to respond to stimuli, reduces personal performance, concentration, and judgment, and causes negative emotional reactions. These effects can lead to accidents. In Taiwan, knowledge about fatigue is still limited. According to a report from the Department of Health (Taipei city government), approximately 30% of office workers in Taiwan (more than 2.6 million people) suffer from chronic fatigue. Furthermore, fatigue is not limited to just workers; it can affect everyone. Fatigue can arise from factors such as insufficient sleep and heavy workloads and may even be attributed to conditions like chronic fatigue syndrome or cancer [1]. If people can understand their fatigue condition well over a long period of time, they can not only adjust their fatigue well but also reduce the occurrence of complications from other diseases and accidents.

Heart rate variability (HRV) is a widely utilized method for assessing levels of fatigue [2–4]. In order to compute HRV indices, many studies initially employ a specialized device to measure the electrocardiogram (ECG) at three specific points, utilizing conductive glue as the conducting medium. One electrode patch is directly attached to the uncovered chest area, minimizing interference from clothing. The other two measurement sites are confined to the chest and hands. Subsequently, peak detection techniques can be applied to identify intervals between successive heartbeats, enabling the derivation of HRV values [5,6]. The ECG was susceptible to power noise and electromagnetic interference (EMI) during the measurements, thus resulting in an inaccurate analysis of the HRV [7]. Power noise and EMI disrupt the ECG signal, distorting it and introducing unwanted signals. This can obscure R-wave peaks crucial for HRV analysis and complicate interval measurement. Furthermore, HRV assessment was vulnerable to external influences. Changes in breathing patterns, increased parasympathetic nerve activity due to relaxation, or variations in current mood could hinder the clear responsiveness of HRV indices to fatigue [8,9]. Factors such as physical activity [10], caffeine and medications [11], stress and emotional state [12], as well as underlying health conditions [13], all have the potential to affect the precision of HRV measurements.

In recent years, optoelectronic and electronic technologies have advanced, and photoplethysmography (PPG) is a commonly used method to determine the condition of blood vessels. With a combination of an appropriate preprocessing of the PPG signal and an artificial intelligence (AI) algorithm, the variables for calculating physiological parameters can be obtained, including heart rate [14,15], blood pressure [16], blood oxygen saturation levels (SpO_2) [17], biometric identification [15], and epileptic seizure detection [18]. Thus, the utilization value of the PPG signal is very high. The measurement of PPG does not require complex algorithms and devices. A PPG signal is convenient to detect, safe, and free of cross-infection. PPG signals provide people with a non-invasive measurement method and are a simple and effective method for monitoring human physiological signals. Although several previous studies adopted PPG to observe the fatigue index [19–21], most of them used PPG to calculate the HRV index and then found the relationship between HRV and fatigue. Thus, even after the use of PPG to calculate HRV, certain problems related to HRV descriptions were still encountered [8,9].

When blood circulation is not smooth, metabolic waste accumulates in blood vessels, stimulates nerve endings, and causes fatigue [22,23]. In such a case, PPG can be adopted to observe the temporal intravascular blood volume changes [24] and assess the microcirculation and intravascular fluid volume [25]. The motivation behind this study was to assess and formulate novel fatigue indices utilizing PPG signals, with a specific focus on analyzing fatigue based on the position of the dicrotic peak. The primary objectives included examining the correlation between various fatigue indices (such as HRV indices and the newly proposed fatigue index) and fatigue levels as measured through questionnaires. This analysis aimed to identify the types of indices that are most appropriate for effectively analyzing and evaluating fatigue.

The aim of this study was to substitute the fatigue index using PPG signals for the subjective data obtained from the (BFI)-Taiwan form and the HRV indices obtained from PPG signals to analyze fatigue and develop a fatigue evaluation system. Commercially available instrumentation (COMGO, Giant Power Technology Biomedical Corp, New Taipei City, Taiwan [26]) was adopted to collect the signals considered in this study. The measurement data were transmitted to the computer through the universal serial bus (USB), and the proposed fatigue evaluation system was implemented using C# code executed in a computer environment. Thus, the system could automatically analyze the fatigue value; these results could be used to further prevent fatigue-related problems.

2. Related Works

Fatigue exerts a profound influence on both physical and mental well-being. Prior research consistently underscores the detrimental implications of fatigue on health [27–29]. Recognizing the critical nature of fatigue assessment, if individuals can gain an extensive comprehension of their fatigue levels over an extended period, they can adeptly regulate their fatigue and potentially curtail the likelihood of complications arising from other ailments and accidents. Consequently, a plethora of subjective questionnaires have been devised to facilitate users' direct comprehension of their fatigue status. Nonetheless, concerns often arise regarding the subjectivity of such questionnaires, raising questions about their objectivity and scientific validation. In response, recent times have witnessed the emergence of diverse methodologies that synergize varied physiological signals with AI technology to comprehensively assess fatigue. The subsequent sections expound on the distinct approaches employed for fatigue evaluation.

2.1. Subjective Fatigue Questionnaires

Subjective fatigue questionnaires involve assessing fatigue levels across various scenarios and timeframes using a series of questions. Below are several commonly used questionnaires for measuring fatigue, accompanied by brief explanations:

A. Brief Fatigue Index (BFI) [30]: A widely employed questionnaire assessing participants' fatigue levels within the previous 24 h;
B. Beck Fatigue Inventory (BFI) [31]: Evaluates subjective fatigue sensations and quality of life, suitable for diverse populations;
C. Fatigue Severity Scale (FSS) [32]: Quantifies the severity of fatigue and helps discern if fatigue impacts daily activities;
D. Multidimensional Fatigue Inventory (MFI) [33]: Assesses fatigue perceptions across various dimensions, including physical, emotional, cognitive, and activity-related aspects;
E. Beijing Fatigue Questionnaire (BFQ) [34]: A Chinese questionnaire gauging the impact of fatigue on quality of life;
F. Fatigue Symptom Inventory (FSI) [35]: Evaluates different fatigue symptoms and impacts, applicable across various medical conditions;
G. Amsterdam Fatigue Questionnaire (AFQ) [36]: Designed for cancer patients, this questionnaire measures the frequency and severity of fatigue.

While subjective fatigue questionnaires are advantageous for assessing fatigue levels, they also possess limitations. These questionnaires directly capture participants' subjective perceptions of fatigue, providing insights into individual fatigue during specific timeframes. However, such subjective assessments can be influenced by participants' emotions and subjective biases, potentially introducing errors. Additionally, linguistic and cultural factors may impact the questionnaires' applicability, requiring cross-cultural adaptation and validation for effectiveness. Importantly, these questionnaires extend beyond office workers, finding relevance among diverse global populations. In Taiwan, for instance, around 30% of over 2.6 million office workers experience chronic fatigue. Yet fatigue transcends workplaces, affecting people worldwide and contributing to health issues and accidents. Understanding individuals' fatigue states supports effective fatigue management and mitigates risks associated with other health conditions. While fatigue measurement questionnaires have strengths, they also face limitations. Reliance on participants' reports may introduce subjective errors due to individual perceptions and emotions. Some questionnaires rely on recalling fatigue experiences, subject to memory biases. Furthermore, lifestyle factors like insufficient sleep or high workloads might not be fully considered, impacting fatigue assessment. Language and cultural nuances may affect questionnaires' applicability, necessitating adaptation and validation across diverse cultures.

In conclusion, fatigue measurement questionnaires offer valuable tools but require careful consideration of their limitations. To comprehensively assess fatigue, integrating objective physiological signals may yield more precise results.

2.2. Objective Physiological Signals

The evaluation of fatigue using objective physiological signals encompasses a range of methods that provide quantifiable insights into the body's response to fatigue. These approaches offer an invaluable alternative to subjective measures and play a pivotal role in unraveling the intricate interplay between fatigue and physiological changes.

Among these methods, heart rate variability (HRV) stands out as a prominent and widely used approach [2–4]. HRV leverages the variations in time intervals between heartbeats to gauge the activity of the autonomic nervous system. As fatigue can exert an influence on autonomic function, HRV serves as a sensitive indicator of fatigue levels and regulatory dynamics.

Skin Conductance [37], another method, involves the measurement of changes in electrical conductivity in response to stress and emotional states. Fatigue-induced alterations in skin conductance provide direct insights into the physiological impact of fatigue on the body's stress response.

Electroencephalogram (EEG) recordings capture the electrical activity of the brain and offer insights into attention, focus, and cognitive states [38,39]. Changes in EEG patterns due to fatigue signify cognitive fatigue and serve as a valuable metric for evaluating mental fatigue. Furthermore, brainwave signal analysis, encompassing various frequencies like alpha, beta, delta, and theta, reveals changes associated with attention, relaxation, and concentration [40]. Brainwave signals furnish an objective measure of cognitive fatigue.

Electromyography (EMG), used to assess muscle fatigue, captures electrical signals generated by muscles during contraction [41]. This method is particularly valuable in studies involving physical tasks and sports-related fatigue, providing objective data on muscle fatigue levels.

Pupillary response analysis involves monitoring changes in pupil size in response to light variations, offering insights into attention and cognitive states [42]. These responses mirror the effects of fatigue on cognitive functioning.

These objective physiological signaling methods transcend the limitations of self-reported questionnaires by providing quantifiable metrics. They bridge the gap between subjective experience and objective assessment, offering a deeper understanding of how fatigue impacts various bodily functions. By decoding these signals, researchers gain crucial insights into the intricate connections between fatigue and physiological responses, facilitating informed interventions and effective management strategies. Among these methods, HRV is extensively utilized in fatigue assessment due to its sensitivity to changes in the autonomic nervous system, which are influenced by fatigue. Fatigue can impact the functionality of the autonomic nervous system, leading to fluctuations in HRV. Consequently, HRV serves as a reliable indicator of an individual's fatigue levels, making it a valuable tool in fatigue evaluation.

HRV can be derived from both ECG [5,6] and PPG signals [43,44]. The ECG measures the electrical activity of the heart, providing precise information about the intervals between consecutive heartbeats. On the other hand, PPG records changes in blood volume and blood flow by analyzing the variations in light absorption or reflection, usually from a fingertip or wrist. Both ECG and PPG can be employed to calculate HRV, which involves analyzing the time intervals between successive heartbeats. HRV is a valuable indicator of the autonomic nervous system's activity and balance, reflecting the dynamic interplay between the sympathetic and parasympathetic branches. By assessing HRV from ECG or PPG signals, researchers gain insights into how the autonomic nervous system responds to various physiological and environmental factors, including fatigue. The choice between ECG and PPG for HRV analysis often depends on the study's objectives, the availability of equipment, and the desired level of accuracy. ECG is considered the gold standard for HRV analysis due to its direct measurement of electrical activity, but PPG offers a more convenient and non-invasive alternative. Both methods contribute significantly to the understanding of fatigue and its physiological implications, enhancing the spectrum of tools available for fatigue assessment and management.

However, the susceptibility of ECG and PPG to power noise and electromagnetic interference (EMI) hampers accurate heart rate variability (HRV) analysis [7,45]. Power noise and EMI disrupt the ECG signal, distorting it and introducing unwanted signals. This can obscure peaks crucial for HRV analysis and complicate interval measurement. EMI further weakens the signal, introduces artifacts, and distorts the ECG and PPG waveforms, undermining HRV calculations. Inaccurate HRV analysis due to these disruptions can misinterpret autonomic nervous system activity, impacting fatigue assessment and physiological insights. The PPG method is relatively easier to implement, as PPG signals can be obtained without the need for electrode patches and typically only require placing a sensor on the skin. This approach is cost-effective and more convenient to execute, making it potentially more straightforward to calculate HRV in certain scenarios. As mentioned above, PPG signals can also be affected by power noise and EMI, leading to signal interference and distortion. To mitigate these interferences and analyze ECG and PPG features, the use of appropriate filters is necessary to ensure that the signals obtained from PPG are stable and accurate.

Even with careful acquisition of ECG or PPG signals and precise HRV calculation, various factors (such as respiration, physical activity, caffeine and medications, stress, and emotional state, as well as underlying health conditions) can influence the accuracy of HRV measurements [8–13]. For instance, physical activity introduces variability as movement and exertion can alter heart rate variability, while respiration patterns, particularly during deep or rapid breathing, can impact HRV measurements.

When blood circulation is obstructed or compromised, metabolic waste products can accumulate within blood vessels, stimulating nerve endings. This condition may lead to a sensation of fatigue. This phenomenon is known as lactic acidosis or tissue hypoxia. During this process, metabolic waste products like lactic acid accumulate in tissues, potentially stimulating pain receptors and affecting nerve transmission, thereby resulting in feelings of fatigue or discomfort [22,23]. The status of blood vessel circulation can be observed using PPG technology to monitor changes in blood volume within vessels [24,25]. Charlton et al. conducted a study to evaluate the efficacy of various features within the PPG pulse wave for assessing mental stress [46]. The findings from their study emphasized that the crest time (duration from pulse onset to peak) and diastole duration (duration from dicrotic notch to pulse end) emerged as viable options for stress assessment. Additionally, the analysis suggested that the radial artery was more suitable for stress assessment compared to the brachial or temporal arteries. Enhancing performance might involve combining crest time and diastole duration with other attributes derived from the second derivative of the PPG, which remains unaffected by heart rate variations. PPG has diverse clinical applications, including physiological monitoring (oxygen saturation, heart rate, blood pressure, respiration), vascular assessment (arterial health, compliance, endothelial function, microvascular flow), and autonomic function evaluation (vasomotor activity, blood pressure, heart rate variability). PPG's pulse wave characterization reveals these associations [47]. Therefore, this study departs from using the HRV method and instead examines the position of the dicrotic peak, which appears to vary under different fatigue states. Thus, the position of the dicrotic peak is used to define the fatigue index.

3. Method

Figure 1 shows the overall workflow of this study. In this study, the subjective fatigue scores were derived from the BFI Taiwan questionnaire, while PPG signals were captured using the COMGO measurement device. Subsequently, to address potential noise interference and individual variations inherent in PPG signals during measurements, a preprocessing step was employed to suppress signal noise and standardize the data. Following preprocessing, the signals underwent the peak detection methods introduced in this paper to identify key points—pulse onset, systolic peak, dicrotic notch, and diastolic peak—for each cycle within the PPG signal. Once these four distinctive points were established for each PPG cycle, the systolic peak was utilized to define the HRV index, whereas the diastolic peak and systolic peak were employed to define the proposed fatigue index. Subsequent to this, the relationship between NHF within the HRV index, the proposed fatigue index, and the subjectively assessed fatigue state gleaned from the questionnaire was evaluated using the correlation coefficient. Utilizing the correlation coefficient, this study determined which subjective fatigue items in the questionnaire exhibit strong correlations with the NHF and the proposed fatigue index. Given the questionnaire's multiple fatigue feedback items, this step aimed to identify those most closely aligned with the NHF and the proposed fatigue index. Subsequently, a linear regression analysis was conducted to establish a model wherein the corresponding subjective fatigue state is the output, while NHF and the proposed fatigue index serve as inputs. This model offers flexibility to predict the subjective fatigue state using either the NHF or the proposed fatigue index. Furthermore, the correlation coefficient was employed to assess the relationships between predicting the subjective fatigue state using either the NHF or the proposed fatigue index and the actual subjective fatigue state. This evaluation helps discern which index is better suited for predicting the subjective fatigue state. The resultant linear regression function was then translated into a C# implementation, giving rise to a real-time fatigue analysis system that facilitates on-the-fly assessment of fatigue levels. Subsequent sections of this paper will provide detailed elaborations on each of these methods.

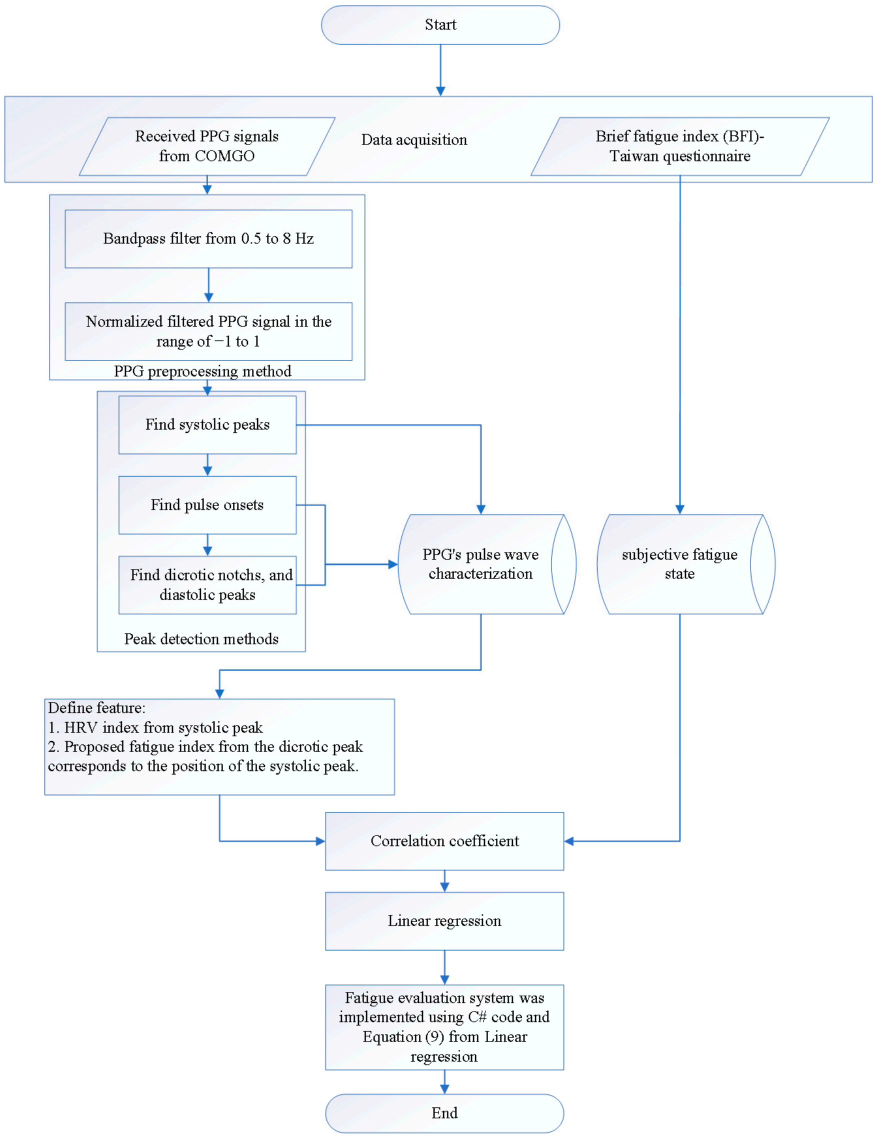

Figure 1. Overall workflow of this study.

3.1. Participants

Sixteen healthy adults (16 males, ages: 22–24) participated in this study. None of the participants had chronic illnesses or sleep disorders. The Institutional Review Board of the National Yang Ming Chiao Tung University approved the experimental protocol (NCTU-REC-109-001F) used in this study. None of the participants were aware of the hypotheses being tested. All of the participants provided their informed consent prior to any experimentation. The experiment took place in the afternoon (2–3 PM). The tester explained the measurement questionnaires: Brief fatigue index (BFI)-Taiwan form [30]. Once the participants understood the content of these questionnaires, they could fill them out easily. Next, the tester explained the operation mode of the cardiovascular measuring instrument and let the participants understand how to use the instrument to measure the PPG signals in order to avoid the possible termination of the experiment caused by the participants' lack of understanding of how to use it. Before measuring the PPG signals, the participants were asked to rest for 5–10 min until they felt relaxed.

This study was to represent an initial exploration of the relationship between novel fatigue indices derived from PPG signals, with a specific emphasis on assessing fatigue based on the position of the dicrotic peak. In the future, we aim to expand the scope of our research by including a broader range of age groups and gender diversities, thereby enhancing the comprehensiveness of our analysis.

3.2. Data Acquisition

Two types of data were considered in this study: behavior data and PPG signals. The behavior data were the subjective data obtained from a brief fatigue index (BFI)-Taiwan questionnaire [30]. The PPG signals were the objective data measured using the COMGO device (Giant Power Technology Biomedical Corp., New Taipei City, Taiwan [26], Taiwan Food and Drug Administration No. 007249) and adopted to develop the objective index for fatigue. Behavior data encompassed subjective assessments of fatigue levels across various situations and time periods through questionnaires. In contrast, PPG signals were employed to capture physiological indices, encompassing HRV indices and a newly proposed fatigue index in this study. The novel fatigue index was defined based on the position of the dicrotic peak. Subsequently, a sequential analysis can be conducted to determine the physiological indices that exhibit correlations with fatigue.

3.2.1. Behavior Data

This study adopted the brief fatigue index (BFI)-Taiwan questionnaire [30] to evaluate the subjective fatigue state. The BFI questionnaire is a simple survey used to assess individuals' fatigue levels in different situations and time periods. Its design aims to rapidly collect participants' subjective fatigue perceptions, allowing for a quick and convenient quantification of their fatigue levels. Additionally, since the participants are all Taiwanese, the questionnaire is more easily understood by them due to its content being tailored to their cultural context. The aim of this study was to determine the type of features that could reflect the fatigue status of the previous day. In the BFI-Taiwan form [30], there were nine questions in all, as shown in Table 1. Each question was assigned a score of 0 to 10 for the subject to choose, and the grading standard is presented in Table 2. The definitions presented in Tables 1 and 2 originate from the BFI-Taiwan form itself [30]. However, considering that the questionnaire is in Chinese, this study has undertaken the task of translating the content into English to facilitate readers' comprehension.

Table 1. Nine questions in the questionnaire.

Item	Questions in BFI-Taiwan Form
1	Current level of fatigue
2	Level of general fatigue in the past 24 h
3	Level of most exhaustion in the past 24 h
4	Fatigue affects the level of general activity in the past 24 h
5	Fatigue affects the level of mood in the past 24 h
6	Fatigue affects the level of walking ability in the past 24 h
7	Fatigue affects the level of Daily work (including going out to work and housework) in the past 24 h
8	Fatigue affects the level of social interaction in the past 24 h
9	Fatigue affects the level of enjoyment of life in the past 24 h

Table 2. Grading standard in BFI-Taiwan Form.

Score	Fatigue State
0	No feeling of fatigue at all
1–3	A little tired (not tired most of the time, but occasionally a little tired)
4–6	Moderately tiring and tolerable (tired for about half the time)
7–9	Quite tired (feeling tired most of the time)
10	Very tired (feeling tired all the time)

3.2.2. PPG Signals

In this study, the COMGO device was used to measure the PPG signals for 2 min at a sampling rate of 200 Hz. In the Taiwanese market, wearable devices with comprehensive physiological sensing are rare. The COMGO device stands out by merging smart health bracelet features and offering various functions. Unlike similar products focusing on heart rate alone, COMGO encompasses blood pressure, oxygen levels, body temperature, ECG, and vascular elasticity monitoring. Utilizing simultaneous finger artery measurements for PPG signals, it transmits data via Bluetooth to a smartphone, then to the cloud via a network (4G, 5G, or Wi-Fi). Portable and compact, COMGO enables convenient and rapid PPG measurements, vital for identifying fatigue-related traits.

3.3. PPG Preprocessing

When measuring PPG signals, it is possible to encounter various types of noise. These noises can originate from multiple sources, including environmental, physiological, and equipment-related factors, resulting in abnormalities or variations in PPG signals [48,49]. Therefore, during the processing and analysis of PPG signals, appropriate data preprocessing and filtering methods are necessary to mitigate the impact of these noises on the results. In this study, the received PPG signals (Figure 2a) were sequentially processed by using a bandpass filter from 0.5 to 8 Hz in order to remove the DC offset and the PPG drift that occurred when the fingers were shaking (Figure 2b) and normalized, which set the value of the filtered PPG signal to be in the range of -1 to 1 (Figure 2c) [50].

Figure 2b shows that the filter frequency between 0.5 Hz and 8 Hz could not only eliminate the drift voltage but also maintain the amplitude of the original signal [50]. The signals at other frequencies would have the same obvious attenuation. After filtering the PPG signal, the mean normalization method was employed for subsequent analysis and comparison. This step aimed to confine the amplitude range of each individual's PPG signal between -1 and 1, thereby addressing the significant data gap [51,52] as outlined by Equation (1):

$$X_{normalize} = 2 \times \frac{x}{x_{max} - x_{min}} \quad (1)$$

where x_{max} indicates the maximum of the filtered PPG signal, and x_{min} represents the minimum of the filtered PPG signal.

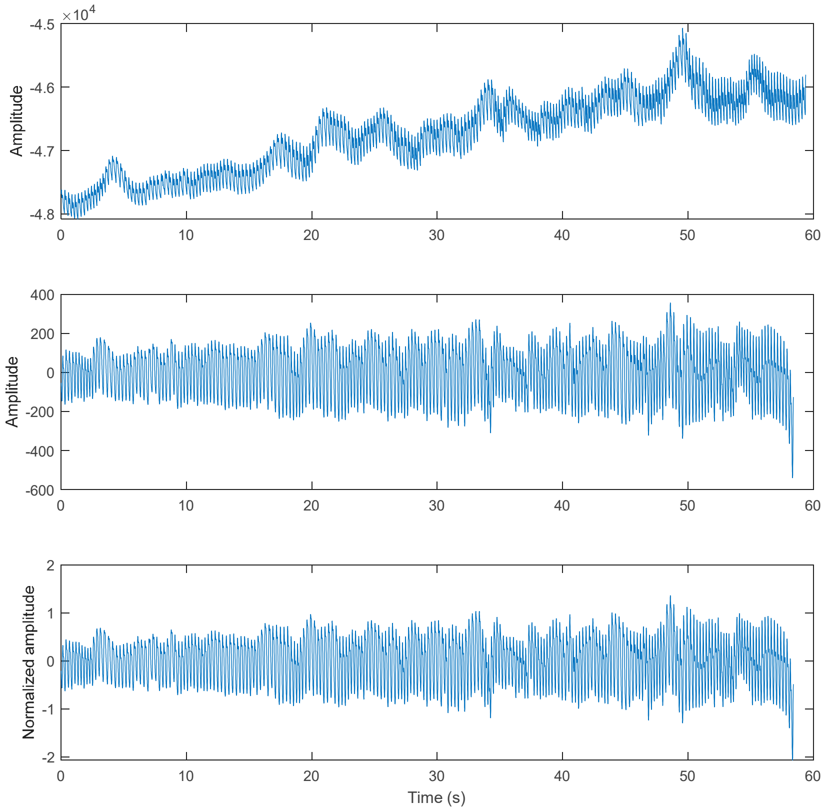

Figure 2. (**a**) Original PPG signal from device. (**b**) Filtered PPG signal after bandpass filter processing. (**c**) Normalized PPG signal.

3.4. Peak Detection Methods

When the preprocessing was completed, the peak of the PPG signal was captured using the proposed peak detection method. The definition of a cycle in the PPG signal was from the beginning of the heart contraction to the next contraction. That is, the time period between two adjacent troughs in each cycle. In order to capture the physiological information from the PPG signal, it was necessary to calculate the positions of the pulse onset, systolic peak, dicrotic notch, and diastolic peak in each cycle.

3.4.1. Systolic Peak

PPG was a continuous and fixed-frequency signal, therefore requiring the definition of how to calculate a computing cycle interval while simultaneously encompassing pulse onset, systolic peak, dicrotic notch, and diastolic peak. The highest peak in a single-cycle PPG signal was the systolic peak. This peak was formed by the direct transmission of the pressure of the cardiac contraction to the end of the measuring device, which resulted in the maximum volume and blood flow in the artery. The systolic peak was a representative feature point in the PPG signal. Furthermore, the cycle had to be defined first to obtain the systolic peak. This study adopted the derivative-based approach by identifying the zero crossing points [53,54] to evaluate the computing cycle as follows:

1. Extract a 10-s normalized PPG signal (Figure 2c) to evaluate the computing cycle;
2. Define a suitable cycle during the 10-s PPG signal. The default calculation cycle is 10 points;
   A. Determine the maximum point *point*(n) within each of the 10 points by using the max function (a MATLAB R2022bfunction).
   B. Evaluate the adjacent maximum point to define it *slope*(n) according to Equations (2) and (3):

$$if\ point(n) < point(n+1),\ slope(n) = 1 \tag{2}$$

$$if\ point(n) \geq point(n+1),\ slope(n) = 0 \tag{3}$$

C. Use the location of *point*(n) corresponding to *slope*(n) = 1 *and slope*(n + 1) = 0 to find the maximum point from *point*(n) to *point*(n) + *size of* cycle. This maximum point is the temple systolic peak.

D. Calculate the average difference among the adjacent temple systolic peaks and then average the estimates divided by the sample rate (200 Hz); this is the heart rate.

E. If the heart rate is smaller than 0.3 or greater than 1.5 s [55], add 5 points to the cycle and go back to Step A.

3. Adopt the calculation cycle for the 2-min normalized PPG signal and obtain the highest peak in each cycle. Thus, the systolic peak is obtained.

3.4.2. Pulse Onset

The lowest peak in a single-cycle PPG signal is the pulse onset. The pulse onset is usually located between the previous diastolic peak and the systolic peak of the next cycle. This study adopted the obtained calculation cycle for the 2-min normalized PPG signal and determined the pulse onset by using the min function (a MATLAB function).

3.4.3. Dicrotic Notch and Diastolic Peak

A dicrotic wave, including the dicrotic notch and the diastolic peak, is the critical duration when the systole and the diastole occur (Figure 3). However, the turning point of the dicrotic wave is not necessarily obvious. The location of the dicrotic wave is affected by many physiological factors and causes the dicrotic wave to be inconspicuous [56], as shown in Figure 3b. In contrast, Figure 3a shows the conspicuous dicrotic wave, and thus, the dicrotic notch and the diastolic peak can be obtained easily.

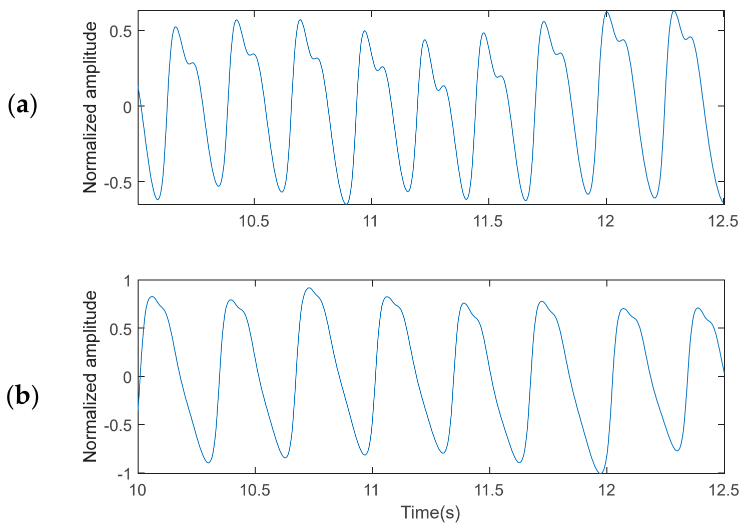

Figure 3. (**a**) Conspicuous dicrotic wave. (**b**) Inconspicuous dicrotic wave.

According to the different conditions of the dicrotic wave, this study proposed two strategies to obtain the dicrotic notch and the diastolic peak as follows:

1. Extract the PPG signal from the cycle of the systolic peak to the cycle of the systolic peak plus half of the time difference between the cycle of the systolic peak and the next cycle of the pulse onset, and calculate the differential signal using the first-order derivatives (Equation (4)):

$$y[n] = x[n] - x[n-1] \tag{4}$$

where $y[n]$ denotes the first-order derivatives of the normalized PPG signal. Next $x[n]$ represents the normalized PPG signal and n refers to the time point. If some values of the first-order derivatives are greater than zero, the locations of zero in the first-order derivatives are the dicrotic notch and the diastolic peak.

2. If no value of the first-order derivatives is greater than zero, the first-order derivatives are adopted to $y[n]$. That is, this study applied the second-order derivatives to the normalized PPG signal. The maximum and minimum of the second-order derivatives were the dicrotic notch and the diastolic peak (Figure 4).

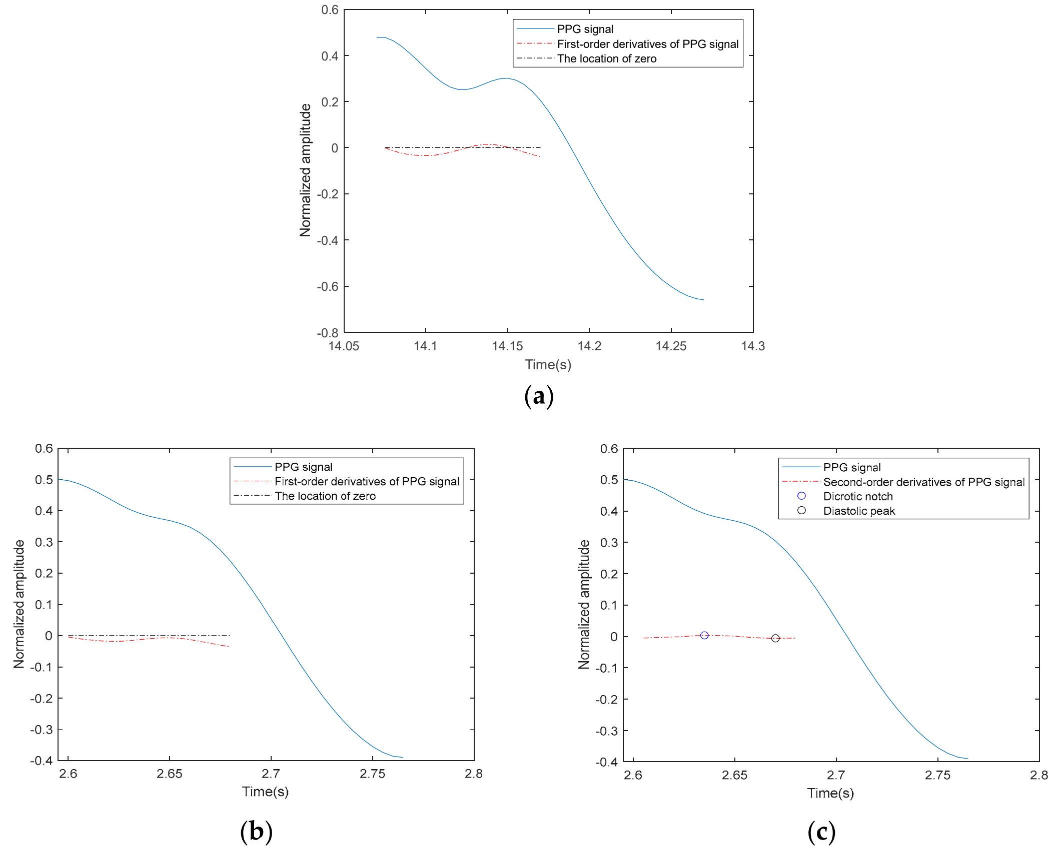

Figure 4. (**a**) Some values of first-order derivatives were greater than zero. (**b**) No value of first-order derivatives was greater than zero. (**c**) Maximum and minimum of second-order derivatives were dicrotic notch and diastolic peak.

3.5. HRV Indices

Some previous studies suggested that the HRV indices can respond to fatigue [2,3,19–21]. Thus, this study also evaluated the relationship between HRV indices and fatigue. The HRV indices were calculated using the R-R interval of the ECG signal [57]. The R-R interval required the tracking of small changes (milliseconds) in the intervals between successive heartbeats (the R peak) in the EEG signal. Furthermore, the R-R interval was similar to the interval between the adjacent systolic peaks of the PPG signal [58,59]. This study adopted the PPG signal to obtain the R-R interval and then evaluated the HRV indices as follows:

1. The R-R interval was calculated according to the interval between the adjacent systolic peaks of the PPG signal, as shown in Figure 5. Each R-R interval responded to the time point of the previous systolic peak;
2. Furthermore, the R-R interval was resampled in this study. The resample function (Signal Processing Toolbox in MATLAB) was used to resample the R-R interval to 250 Hz;

3. The resampled R-R interval was subjected to the fast Fourier transform with a Hamming window. This study focused on three frequency bands: the VLF (0.003–0.04 Hz), LF (0.04–0.15 Hz), and HF (0.15–0.4 Hz) [60]. The powers of the LF and HF were normalized by the total power minus the power of the VLF, representing the components in normal units (NLF and NHF) as follows:

$$\mathrm{NLF} = \frac{\mathrm{LF}}{(\mathrm{totoal\ power} - \mathrm{VLF})} \times 100 \tag{5}$$

$$\mathrm{NHF} = \frac{\mathrm{HF}}{(\mathrm{totoal\ power} - \mathrm{VLF})} \times 100 \tag{6}$$

where $total\ power = LF + HF + VLF$. The representation in normalized units tended to minimize the effects of the changes in total power on the values of LF and HF [61] and attempted to separate out the influence of the sympathetic and parasympathetic nervous systems on the sympathovagal balance [62]. The sympathovagal balance was calculated by using the ratio of the LF power to the HF power (LF/HF ratio);
4. Sympathetic and parasympathetic activity were closely linked to emotion [63,64]. The higher sympathetic tone (*NLF*) responded to the tense, anxious, and excited emotion, and the higher parasympathetic tone (*NHF*) responded to the tired, calm, and happy emotion [65]. In addition, Jeong et al. suggested that [4] the index of the parasympathetic nerve (NHF) was more obvious than that of the sympathetic nerve (NLF) with respect to the fatigue index. Thus, this study attempted to evaluate the relationship between NHF and fatigue. In addition, the range of values for NHF was from 0 to 100. The range of subjective fatigue and the proposed fatigue index were from 0 to 10. The range of NHF values had been changed to 0 to 10.

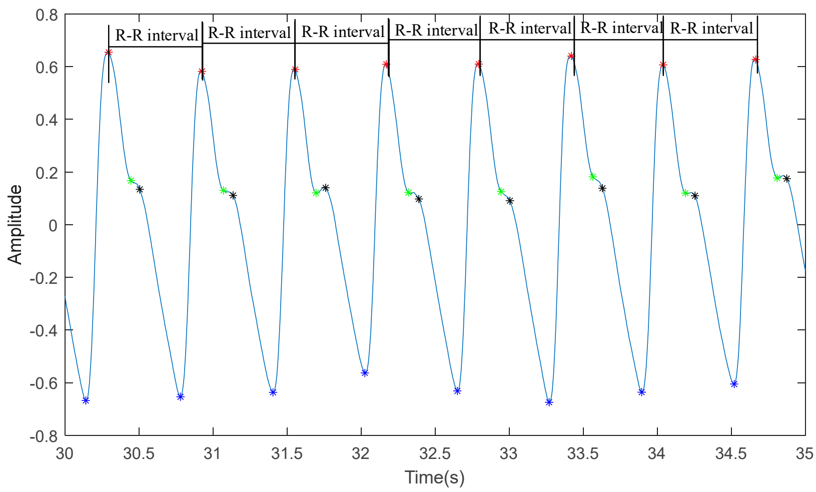

Figure 5. The R-R interval is defined as the time interval between adjacent systolic peaks (red *).

3.6. Fatigue Index

When blood circulation encounters obstruction, there's a potential for metabolic waste products to accumulate within blood vessels, subsequently stimulating nerve endings. This scenario necessitates the heart to exert more effort in processing the accumulated metabolic waste, thereby resulting in fatigue [22,23]. From the perspective of the overall blood circulation, if the heart has to overcome excessive vascular pressure during its contraction, this could impede the propagation of pressure waves during cardiac contractions, consequently leading to a relatively higher position of the dicrotic peak. Therefore, a relatively higher position of the dicrotic peak may suggest alterations associated with fatigue [66]. Consequently, this study employed the position of the dicrotic peak to formulate the fatigue index (as depicted in Figure 6) using the following approach:

1. Obtain the vertical height of the systolic peak as x, and define the half of x as the zero. Then, the new range is defined from zero to the systolic peak and mapped to 0–10, which corresponds to the score of the brief fatigue index (BFI)-Taiwan form [30];
2. Calculate the position of the dicrotic peak from the defined range in each cycle. The position is one fatigue index in one cycle of the PPG signal;
3. Calculate all the fatigue indices during the 2-min measurement, and then calculate the average of all of the fatigue indices. Thus, the average fatigue index is defined to represent the objective index of fatigue for the participants.

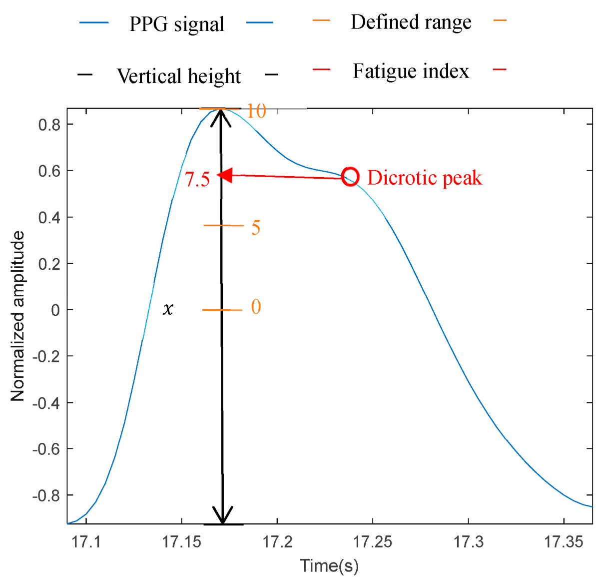

Figure 6. Definition of fatigue index.

3.7. Linear Regression

A linear regression model is a regression analysis that estimates the relationship between one or more independent variables and dependent variables. The common linear regression is a least-squares fit, which can fit both lines and polynomials, among other linear models [67,68].

This study utilized linear regression to examine the association between the subjective fatigue state assessed using the brief fatigue index (BFI)-Taiwan form [30], the NHF, and the proposed fatigue index. Additionally, linear regression was employed to predict the fatigue state from the BFI-Taiwan form, employing distinct predictors (NHF and the proposed fatigue index). This approach aimed to develop a model that leveraged physiological indices for the prediction of fatigue levels. The regression model could be described as follows:

$$\mathcal{Y} = a + b\mathrm{X} \tag{7}$$

where $\mathcal{Y}$ denotes the subjective fatigue state, while X can be NHF or the proposed fatigue index. The regression coefficients a and b were determined using the MATLAB function "regress" (Statistics Toolbox), which minimized the sum of the squared residuals of the model.

3.8. Correlation Coefficient

The correlation coefficient between two random variables serves as an indicator of their degree of linear interdependence. Pearson's correlation coefficient is a prevalent technique for quantifying a linear correlation [69]. It gauges both the intensity and direction of the relationship between two variables by assigning a numerical value between −1 and 1, as shown in Equation (8):

$$r = \frac{\sum_{i=1}^{n}\left(X_i - \overline{X}\right)\left(Y_i - \overline{Y}\right)}{\sqrt{\sum_{i=1}^{n}\left(X_i - \overline{X}\right)^2}\sqrt{\sum_{i=1}^{n}\left(Y_i - \overline{Y}\right)^2}} \quad (8)$$

where X_i and Y_i denotes the data points of two variables, and each variable has n scalar observations. $\overline{X}$ and $\overline{Y}$ represent the mean of two variables. In addition to its application in linear regression within this study, Pearson's correlation coefficient can be effectively employed to measure the relationship between two variables. This encompasses various scenarios, such as comparing the estimated subjective fatigue state obtained through linear regression and the proposed fatigue index with the actual subjective fatigue state, evaluating the connection between NHF and the actual subjective fatigue state, and investigating the correlation between the proposed fatigue index and the real subjective fatigue state.

3.9. Fatigue Evaluation System

In this study, the proposed fatigue evaluation system was implemented using C# code that can be executed within a computer environment. Users are required to measure PPG signals using the COMGO device and subsequently transfer the collected data to the system on a computer via USB. Following this, users have the option to input their name in the designated field labeled 'please enter a name' and upload the recorded PPG file by activating the 'Open file and Test' button (as depicted in Figure 7). Subsequently, the system automatically analyzes the fatigue index and displays the corresponding information, including the name and fatigue index, in a table. If the fatigue index, as elaborated in Section 3.6, exceeds a threshold of 6, the system provides a reminder to the participants to take a rest.

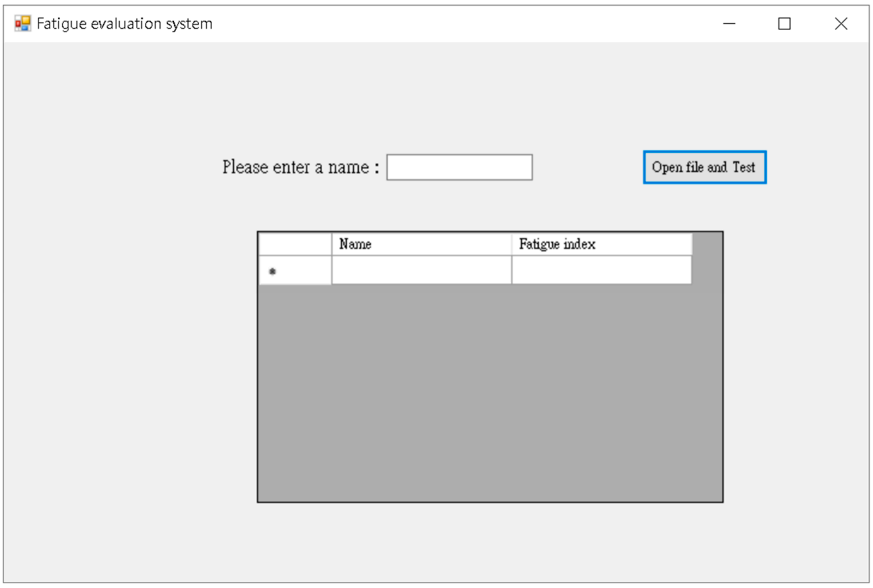

Figure 7. Fatigue evaluation system developed in this study.

4. Results

4.1. Performance of PPG Peak Detection and Proposed Features for Fatigue Index

This study introduced PPG preprocessing and peak detection methods. Figure 8 illustrates the performance of the PPG preprocessing and peak detection techniques employed in this study. The outcomes demonstrate the accurate detection of pulse onset, systolic peak, dicrotic notch, and diastolic peak utilizing the proposed method. This study proposed features for the fatigue index based on the PPG signal. This pattern was observed in our recording data, where the different amplitudes of diastolic peaks responded to different fatigue conditions. The development of the fatigue index was based on the amplitude of diastolic peaks (Figure 6). Figure 8 shows that the different locations of the diastolic peak could represent the fatigue index.

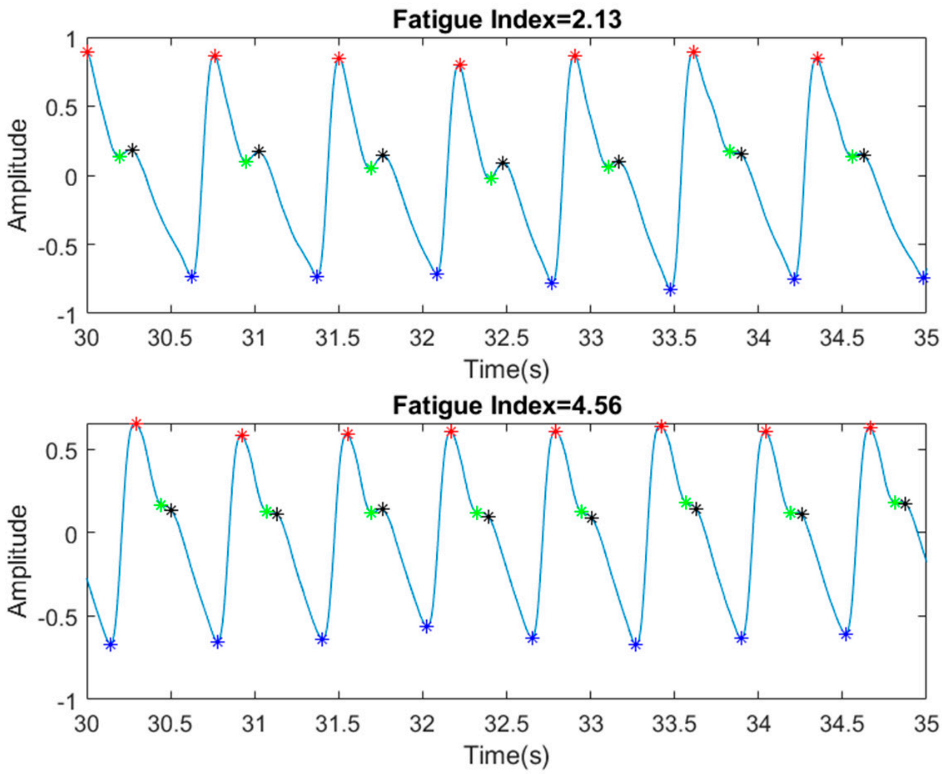

Figure 8. The different locations of the diastolic peak could represent the fatigue index from two samples.

4.2. Data Distribution of Subjective Fatigue State, NHF, and Proposed Fatigue Index

In all, 16 healthy adults participated in this study. The data considered in this study included the subjective fatigue state obtained from the BFI-Taiwan form, the objective NHF, and the proposed fatigue index estimated from the PPG signals. Figure 9 shows the data distribution of the subjective fatigue state, NHF, and the proposed fatigue index of 16 healthy adults (histogram function in MATLAB). This study employed the Anderson-Darling test (adtest function, statistics, and machine learning toolbox in MATLAB), a statistical method, to determine if a given dataset is drawn from a normal distribution. The Anderson-Darling test assesses the fit of the data to a theoretical normal distribution by considering both the mean and the variance of the data. It provides a quantitative measure of how well the observed data aligns with the expected distribution, allowing researchers to make informed judgments about the normality of the dataset under examination [70]. In MATLAB, the "adtest" function was utilized as a means of testing the null hypothesis that the data within the vector "x" originated from a population characterized by a normal distribution. The result h returned by the adtest function was 1 if the test rejected the null hypothesis and then indicated that x was not from a population with a normal distribution. Except for questions (3), (6), (8), and (9) and the proposed fatigue index, most of the data had a normal distribution (h = 0).

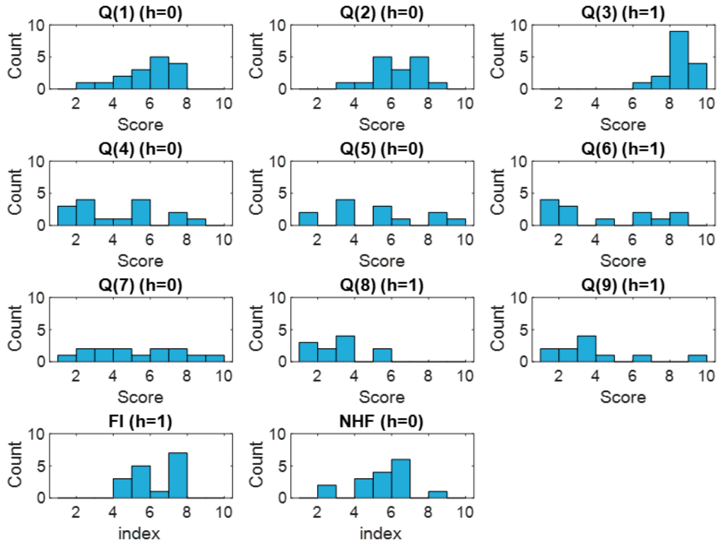

Figure 9. Data distribution of subjective fatigue state, NHF, and proposed fatigue index.

4.3. Relationship among Subjective Fatigue State, NHF, and Proposed Fatigue Index

Figure 10 shows the scatter plot for three datasets: the subjective fatigue state, the NHF, and the proposed fatigue index. Because the aim of this study was to substitute the fatigue index obtained using PPG signals for the subjective data obtained from the (BFI)-Taiwan form and the HRV indices estimated from PPG signals to analyze fatigue, the last two rows of the scatter plot shown in Figure 10 were further explored; they revealed a line relationship between the questions from the BFI-Taiwan form and the proposed fatigue index. Thus, this study adopted Pearson's correlation coefficient to evaluate the relationship among the subjective fatigue state, NHF, and the proposed fatigue index, as shown in Figure 11. The results revealed that only two questions were related to the proposed fatigue index: (2) Level of general fatigue in the past 24 h ($r = 0.8743$) and (3) Level of being most exhausted in the past 24 h ($r = 0.5328$).

In contrast, NHF had a low correlation for all nine questions ($r = -0.1510 \sim 0.4787$). The reason why NHF was unable to respond to fatigue was that the participants adjusted their breathing and the parasympathetic nerve effectively deepened, or the influence of the current mood [8,9]. Previous research suggested that irregular respiration can change sympathovagal activities or their balances, as reflected in the HRV indices [71–75]. Lin et al. also showed that controlled breathing may be effective in controlling nausea and enhancing autonomic function by decreasing sympathetic activity and increasing parasympathetic activity [9].

The degrees of subjective fatigue in the past 24 h could be represented by two questions (2) and (3) (Figure 11) and related to the proposed fatigue index using the PPG signals. This study attempted to average the scores for questions (2) and (3) in the BFI-Taiwan form to represent the revised subjective fatigue state of the participants. In addition, this study adopted linear regression (the regress function of the statistics toolbox in MATLAB) to estimate the relationship between the revised subjective fatigue state and the proposed fatigue index and NHF using PPG signals (Figure 12). The results shown in Figure 12 revealed that Pearson's correlation coefficient between the revised subjective fatigue state and the proposed fatigue index was 0.907 and represented a high positive correlation. Therefore, it could be suggested that the proposed fatigue index was positively correlated with the fatigue level felt by the participants. In contrast, the linear regression of NHF relative to the revised subjective fatigue was low ($r = 0.14875$). This observation corresponds to the trends depicted in Figures 10 and 11, indicating a limited correlation between NHF and the subjective fatigue state. On the other hand, the fatigue index introduced in this study, derived from the position of the dicrotic peak, demonstrates a robust connection with the subjective fatigue state. While earlier literature has suggested a link between NHF and fatigue [2–4], it is important to note that numerous studies have underscored the influence of diverse factors (such as respiration, physical activity, caffeine and medications, stress and emotional state, and underlying health conditions) on the accuracy of HRV measurements [8–13]. In contrast, the fatigue index proposed in this paper, relying on the PPG dicrotic peak's position, aligns with prior research highlighting the effectiveness of various PPG pulse wave features in assessing mental states [46,47]. Moreover, it resonates with the broad range of physiological monitoring applications encompassing oxygen saturation, heart rate, blood pressure, respiration for pulse wave characterization, arterial health assessment, compliance, endothelial function, and microvascular flow for vascular evaluation, as well as vasomotor activity and heart rate variability for autonomic function assessment. This demonstrates that PPG signals extend beyond their role in HRV or heart rhythm assessment, incorporating a diverse array of implications within their waveform characteristics.

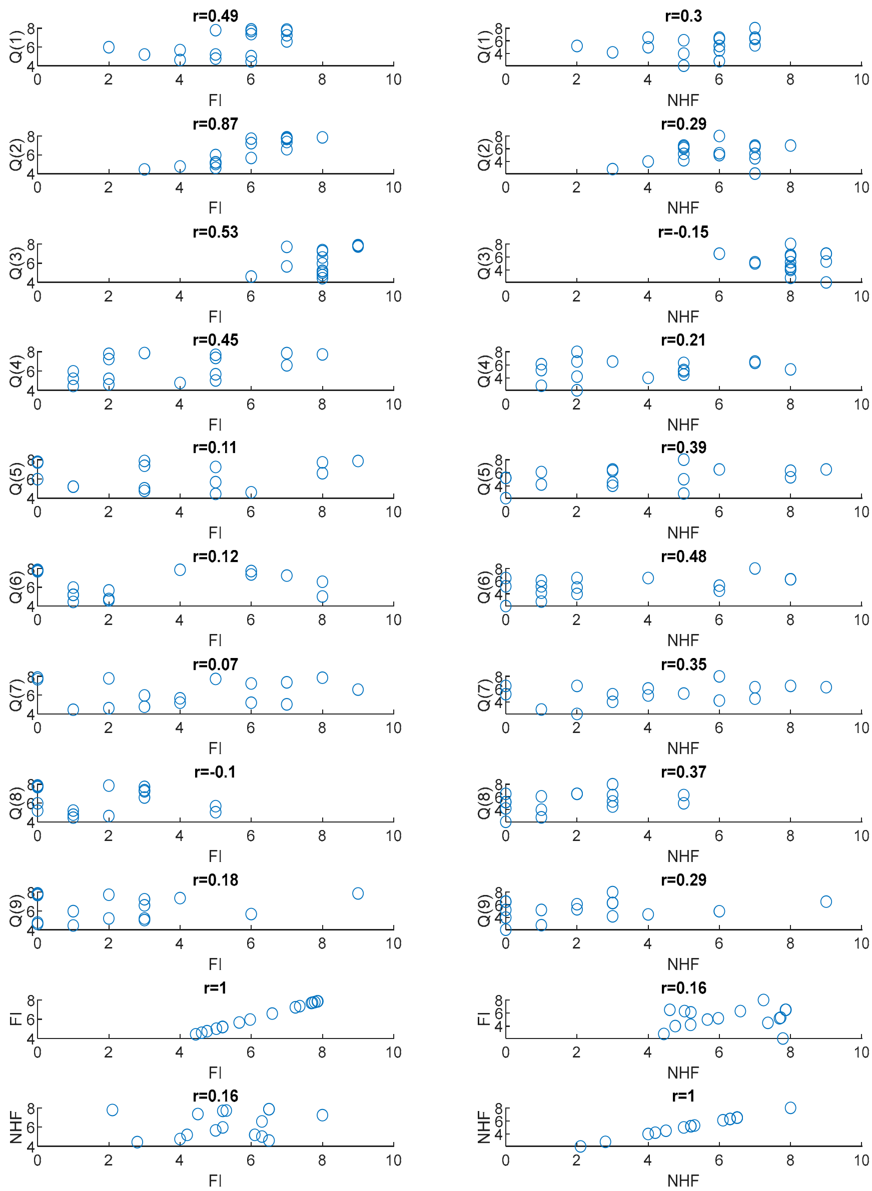

Figure 10. Scatter plot for three data items: subjective fatigue state, NHF, and proposed fatigue index. Q (Question) and FI (Fatigue index). The nine rows of the scatter plot were used to represent the relationship among questions from BFI-Taiwan form, NHF, and proposed fatigue index.

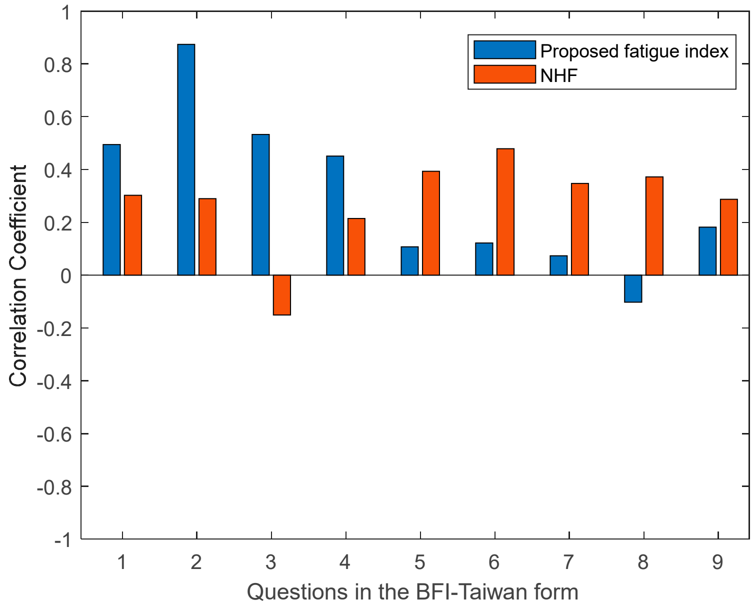

Figure 11. Relationship among subjective fatigue state, NHF, and proposed fatigue index.

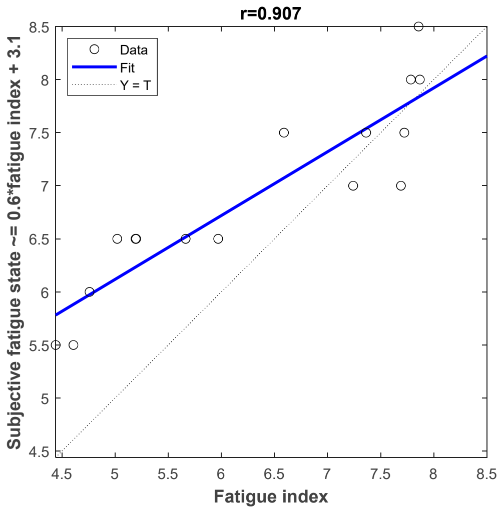

(**a**)

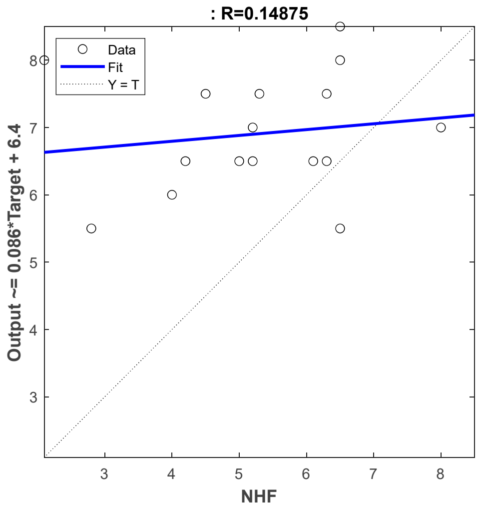

(**b**)

Figure 12. Relationship between subjective fatigue state and proposed fatigue index and NHF using PPG signals using linear regression. (**a**) Linear regression between subjective fatigue state and proposed fatigue index. (**b**) Linear regression between subjective fatigue state and NHF.

The results shown in Figure 12 revealed that the subjective fatigue state could be obtained by Equation (9) using the proposed fatigue index using the PPG signals:

$$\text{Subjective fatigue state} = 0.6 \times \text{fatigue index} + 3.1 \quad (9)$$

4.4. Fatigue Evaluation System

This study implemented PPG processing, peak detection method, fatigue index, and Equation (9) using C# in a computer environment. The measurement file from COMGO was transmitted and saved to the computer through the USB. The participants could enter their names and upload the measurement file by pressing the button "Open file and Test" (Figure 7). The system then automatically analyzed the fatigue index and reminded the participants to take rest if the fatigue index was greater than 6 (Figure 13).

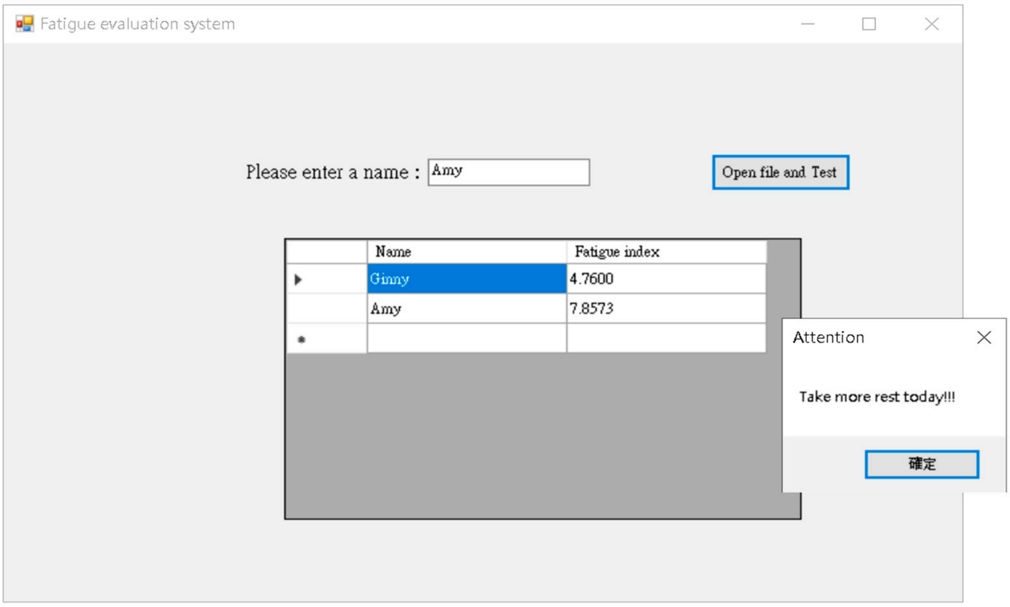

Figure 13. Fatigue evaluation system in this study. The system reminded the subject to take rest if the fatigue index was greater than 6. The 確認 in the 'Attention' window indeed means to confirm the content.

5. Conclusions

This study proposes a novel fatigue index derived from PPG signals, with a specific focus on the position of the dicrotic peak. The proposed fatigue index is utilized to replace subjective data collected through the (BFI)-Taiwan form and the HRV indices obtained from PPG signals in order to evaluate fatigue levels. This research departs from traditional approaches by formulating the fatigue index based on distinct PPG waveform characteristics rather than relying on HRV. Additionally, a comparative analysis is conducted to examine the relationship between the fatigue index derived from PPG waveform characteristics, HRV, and the subjective fatigue assessment in the BFI form. The study also proposes PPG preprocessing and peak detection techniques. The findings demonstrate a robust correlation between the scores of questions in the BFI-Taiwan form and the proposed fatigue index. Of particular significance is the notable correlation observed between two specific questions and the proposed fatigue index: (2) Level of general fatigue in the past 24 h ($r = 0.8743$) and (3) Level of most exhaustion in the past 24 h ($r = 0.5328$). However, the correlation with HRV (HF) remains moderate. As a result, this investigation calculates an average of the scores from questions (2) and (3) in the BFI-Taiwan form to represent participants revised subjective fatigue states. Through the application of Equation (9) with the proposed fatigue index derived from PPG signals, a strong correlation ($r = 0.907$) is established, validating the potential effectiveness of Equation (9). This equation can seamlessly integrate into a C# framework to establish a comprehensive fatigue evaluation system, thereby offering valuable insights for individuals seeking to effectively address fatigue-related concerns. The incorporation of timely reminders serves to alert users when their index surpasses a predefined threshold, thereby cultivating heightened awareness of their physical well-being. Moreover, this study emphasizes that PPG signals surpass their traditional role in HRV, or heart rhythm assessment, encompassing a diverse range of implications within their waveform characteristics.

This study possesses three primary limitations, each offering opportunities for future research enhancement. Firstly, the effect estimates utilized in the adopted approach relied on a relatively modest sample size comprising only 16 healthy adults. To bolster the statistical robustness, expanding participant numbers and encompassing diverse age groups and genders would be advisable. Furthermore, integrating deep learning techniques for estimating fatigue states could introduce advanced analytical capabilities. Secondly, it is plausible that there exist additional factors beyond those addressed in this study that could impact fatigue state prediction. Elements like climatic variations, BMI, age, gender, and others may also exert influence. Consequently, future investigations should consider the inclusion of these variables to foster a more comprehensive grasp of the subject matter. Thirdly, alternate equipment alternatives, such as Doppler ultrasound machines, offer the capacity to visualize specific arteries and their blood flow dynamics through dynamic imaging. By engaging diverse measurement devices, it may be feasible to scrutinize corresponding vascular conditions or capture finer PPG-related features. Delving into the utilization of different measurement tools in forthcoming research would contribute valuable insights, potentially unveiling supplementary features and augmenting the precision of fatigue state prediction within our study.

Author Contributions: Conceptualization, Y.-X.C. and C.-L.L.; methodology, Y.-X.C.; software, Y.-X.C. and C.-L.L.; validation, C.-K.T., J.-T.K., C.-J.W., S.-H.C., L.-J.K., Y.-S.H. and C.-L.L.; formal analysis, C.-K.T. and J.-T.K.; investigation, S.-H.C. and L.-J.K.; data curation, J.-T.K., C.-J.W. and Y.-S.H.; writing—original draft preparation, Y.-X.C. and C.-L.L.; writing—review and editing, C.-L.L.; supervision, C.-L.L. All authors have read and agreed to the published version of the manuscript.

Funding: This work was supported, in part, by the Aiming for the Talent Cultivation Project of the Ministry of Education of Taiwan. Further support came from the Aiming for the Talent Cultivation Project of the Ministry of Education of Taiwan and the Program funded by the National Science and Technology Council of Taiwan under grant number MOST 111-2221-E-131-030.

Data Availability Statement: The datasets used and/or analyzed during the current study available from the corresponding author on reasonable request.

Conflicts of Interest: The authors declare no conflict of interest.

References

1. Bennett, B.; Goldstein, D.; Friedlander, M.; Hickie, I.; Lloyd, A. The experience of cancer-related fatigue and chronic fatigue syndrome: A qualitative and comparative study. *J. Pain Symptom Manag.* **2007**, *34*, 126–135. [CrossRef]
2. Al-Libawy, H.; Al-Ataby, A.; Al-Nuaimy, W.; Al-Taee, M.A. HRV-Based Operator Fatigue Analysis and Classification Using Wearable Sensors. In Proceedings of the 2016 13th International Multi-Conference on Systems, Signals & Devices (SSD), Leipzig, Germany, 21–24 March 2016; pp. 268–273.
3. Napieralski, A.; Ciota, Z.; Martinez, A.; De Mey, G.; Cabestany, J. *Mixed Design of Integrated Circuits and Systems*; Springer Science & Business Media: Berlin/Heidelberg, Germany, 2012.
4. Jeong, I.C.; Lee, D.H.; Park, S.W.; Ko, J.I.; Yoon, H.R. Automobile Driver's Stress Index Provision System that Utilizes Electrocardiogram. In Proceedings of the 2007 IEEE Intelligent Vehicles Symposium, Istanbul, Turkey, 13–15 June 2007; pp. 652–656.
5. Mali, B.; Zulj, S.; Magjarevic, R.; Miklavcic, D.; Jarm, T. Matlab-based tool for ECG and HRV analysis. *Biomed. Signal Process. Control* **2014**, *10*, 108–116. [CrossRef]
6. Karthikeyan, P.; Murugappan, M.; Yaacob, S. Detection of human stress using short-term ECG and HRV signals. *J. Mech. Med. Biol.* **2013**, *13*, 1350038. [CrossRef]
7. Wannenburg, J.; Malekian, R.; Hancke, G.P. Wireless capacitive-based ECG sensing for feature extraction and mobile health monitoring. *IEEE Sens. J.* **2018**, *18*, 6023–6032. [CrossRef]
8. Katona, P.G.; Jih, F. Respiratory sinus arrhythmia: Noninvasive measure of parasympathetic cardiac control. *J. Appl. Physiol.* **1975**, *39*, 801–805. [CrossRef]
9. Lin, C.-L.; Jung, T.-P.; Chuang, S.-W.; Duann, J.-R.; Lin, C.-T.; Chiu, T.-W. Self-adjustments may account for the contradictory correlations between HRV and motion-sickness severity. *Int. J. Psychophysiol.* **2013**, *87*, 70–80. [CrossRef] [PubMed]
10. Rennie, K.L.; Hemingway, H.; Kumari, M.; Brunner, E.; Malik, M.; Marmot, M. Effects of moderate and vigorous physical activity on heart rate variability in a British study of civil servants. *Am. J. Epidemiol.* **2003**, *158*, 135–143. [CrossRef] [PubMed]
11. Ulanovsky, I.; Haleluya, N.; Blazer, S.; Weissman, A. The effects of caffeine on heart rate variability in newborns with apnea of prematurity. *J. Perinatol.* **2014**, *34*, 620–623. [CrossRef]
12. McCraty, R.; Atkinson, M.; Tiller, W.A.; Rein, G.; Watkins, A.D. The effects of emotions on short-term power spectrum analysis of heart rate variability. *Am. J. Cardiol.* **1995**, *76*, 1089–1093. [CrossRef]
13. Tiwari, R.; Kumar, R.; Malik, S.; Raj, T.; Kumar, P. Analysis of heart rate variability and implication of different factors on heart rate variability. *Curr. Cardiol. Rev.* **2021**, *17*, 74–83. [CrossRef]
14. Temko, A. Accurate heart rate monitoring during physical exercises using PPG. *IEEE Trans. Biomed. Eng.* **2017**, *64*, 2016–2024. [CrossRef]

15. Biswas, D.; Everson, L.; Liu, M.; Panwar, M.; Verhoef, B.-E.; Patki, S.; Kim, C.H.; Acharyya, A.; Van Hoof, C.; Konijnenburg, M.; et al. CorNET: Deep learning framework for PPG-based heart rate estimation and biometric identification in ambulant environment. *IEEE Trans. Biomed. Circuits Syst.* **2019**, *13*, 282–291. [CrossRef] [PubMed]
16. Fortino, G.; Giampà, V. PPG-Based Methods for Non Invasive and Continuous Blood Pressure Measurement: An Overview and Development Issues in Body Sensor Networks. In Proceedings of the 2010 IEEE International Workshop on Medical Measurements and Applications, Ottawa, ON, Canada, 30 April–1 May 2010; pp. 10–13.
17. Bagha, S.; Shaw, L. A real time analysis of PPG signal for measurement of SpO_2 and pulse rate. *Int. J. Comput. Appl.* **2011**, *36*, 45–50.
18. Vandecasteele, K.; De Cooman, T.; Gu, Y.; Cleeren, E.; Claes, K.; Van Paesschen, W.; Van Huffel, S.; Hunyadi, B. Automated epileptic seizure detection based on wearable ECG and PPG in a hospital environment. *Sensors* **2017**, *17*, 2338. [CrossRef] [PubMed]
19. Sikander, G.; Anwar, S. Driver fatigue detection systems: A review. *IEEE Trans. Intell. Transp. Syst.* **2018**, *20*, 2339–2352. [CrossRef]
20. Choi, U.-S.; Kim, K.-J.; Lee, S.-S.; Kim, K.-S.; Kim, J. A Simple Fatigue Condition Detection Method by Using Heart Rate Variability Analysis. In *Advances in Parallel and Distributed Computing and Ubiquitous Services: UCAWSN & PDCAT 2015*; Springer: Berlin/Heidelberg, Germany, 2016; pp. 203–208.
21. Honiball, J.R.; Vandenheever, D. The development of a PPG and in-ear EEG device for application in fatigue measurement. *Am. J. Sci. Eng.* **2022**, *3*, 7–17. [CrossRef]
22. Jang, S.H.; Kim, K.H. Effects of self-foot reflexology on stress, fatigue and blood circulation in premenopausal middle-aged women. *J. Korean Acad. Nurs.* **2009**, *39*, 662–672. [CrossRef]
23. Pitcher, J.B.; Miles, T.S. Influence of muscle blood flow on fatigue during intermittent human hand-grip exercise and recovery. *Clin. Exp. Pharmacol. Physiol.* **1997**, *24*, 471–476. [CrossRef]
24. Kao, Y.-H.; Chao, P.C.-P.; Wey, C.-L. A PPG Sensor for Continuous Cuffless Blood Pressure Monitoring with Self-Adaptive Signal Processing. In Proceedings of the 2017 International Conference on Applied System Innovation (ICASI), Sapporo, Japan, 13–17 May 2017; pp. 357–360.
25. Sahni, R. Noninvasive monitoring by photoplethysmography. *Clin. Perinatol.* **2012**, *39*, 573–583. [CrossRef]
26. Tseng, C.-K.; Chao, S.H.; Hwang, Y.S.; Kau, L.J.; Lin, C.L.; Chen, K.C.; Yin, W.H.; Wang, S.F.; Chen, Y.X. Application of A Minimized Wearable Device Combined with SpO_2 and ECG Sensors to Detect Stenosis or Occlusion of Arteriovenous Fistula/Graft, Progression of Arteriosclerosis and Arrhythmia. In Proceedings of the 2018 7th International Symposium on Next Generation Electronics (ISNE), Taipei, Taiwan, 7–9 May 2018; pp. 1–4.
27. Kryger, M.H.; Roth, T.; Dement, W.C. *Principles and Practice of Sleep Medicine E-Book: Expert Consult-Online and Prin*; Elsevier Health Sciences: Amsterdam, The Netherlands, 2010.
28. Åkerstedt, T.; Gillberg, M. Subjective and objective sleepiness in the active individual. *Int. J. Neurosci.* **1990**, *52*, 29–37. [CrossRef]
29. Eldadah, B.A. Fatigue and fatigability in older adults. *PM&R* **2010**, *2*, 406–413.
30. Yang, H.-L.; Chen, X.-P.; Lee, K.-C.; Fang, F.-F.; Chao, Y.-F. The effects of warm-water footbath on relieving fatigue and insomnia of the gynecologic cancer patients on chemotherapy. *Cancer Nurs.* **2010**, *33*, 454–460. [CrossRef]
31. Beck, A.T.; Steer, R.A.; Carbin, M.G. Psychometric properties of the Beck Depression Inventory: Twenty-five years of evaluation. *Clin. Psychol. Rev.* **1988**, *8*, 77–100. [CrossRef]
32. Krupp, L.B.; LaRocca, N.G.; Muir-Nash, J.; Steinberg, A.D. The fatigue severity scale: Application to patients with multiple sclerosis and systemic lupus erythematosus. *Arch. Neurol.* **1989**, *46*, 1121–1123. [CrossRef]
33. Smets, E.; Garssen, B.; Bonke, B.D.; De Haes, J. The Multidimensional Fatigue Inventory (MFI) psychometric qualities of an instrument to assess fatigue. *J. Psychosom. Res.* **1995**, *39*, 315–325. [CrossRef]
34. Wu, C.; Liu, Z.; Zhang, Y.; Li, J.; Wang, D. Validity and reliability of Chinese version of fatigue impact scale in cerebral infarction patients. *Neural Regen. Res.* **2008**, *3*, 177–181.
35. Okuyama, T.; Akechi, T.; Kugaya, A.; Okamura, H.; Imoto, S.; Nakano, T.; Mikami, I.; Hosaka, T.; Uchitomi, Y. Factors correlated with fatigue in disease-free breast cancer patients: Application of the Cancer Fatigue Scale. *Support. Care Cancer* **2000**, *8*, 215–222. [CrossRef]
36. Cella, D.; Lai, J.S.; Chang, C.H.; Peterman, A.; Slavin, M. Fatigue in cancer patients compared with fatigue in the general United States population. *Cancer* **2002**, *94*, 528–538. [CrossRef]
37. Bundele, M.M.; Banerjee, R. Detection of Fatigue of Vehicular Driver Using Skin Conductance and Oximetry Pulse: A Neural Network Approach. In Proceedings of the 11th International Conference on Information Integration and Web-Based Applications & Services, Kuala Lumpur, Malaysia, 14 December 2009; pp. 739–744.
38. Zhao, C.; Zhao, M.; Liu, J.; Zheng, C. Electroencephalogram and electrocardiograph assessment of mental fatigue in a driving simulator. *Accid. Anal. Prev.* **2012**, *45*, 83–90. [CrossRef]
39. Trejo, L.J.; Kubitz, K.; Rosipal, R.; Kochavi, R.L.; Montgomery, L.D. EEG-based estimation and classification of mental fatigue. *Psychology* **2015**, *06*, 572–589. [CrossRef]
40. Chen, C.-L.; Liao, C.-Y.; Chen, R.-C.; Tang, Y.-W.; Shih, T.-F. Bus Drivers Fatigue Measurement Based on Monopolar EEG. In *Intelligent Information and Database Systems: 9th Asian Conference, ACIIDS 2017, Kanazawa, Japan, 3–5 April 2017*; Part II 9; Springer: Berlin/Heidelberg, Germany, 2017; pp. 308–317.

41. Viitasalo, J.H.; Komi, P.V. Signal characteristics of EMG during fatigue. *Eur. J. Appl. Physiol. Occup. Physiol.* **1977**, *37*, 111–121. [CrossRef]
42. De Rodez Benavent, S.A.; Ygaard, G.O.; Harbo, H.F.; Tønnesen, S.; Sowa, P.; Landrø, N.I.; Wendel-Haga, M.; Etholm, L.; Nilsen, K.B.; Drolsum, L.; et al. Fatigue and cognition: Pupillary responses to problem-solving in early multiple sclerosis patients. *Brain Behav.* **2017**, *7*, e00717. [CrossRef] [PubMed]
43. Bhowmik, T.; Dey, J.; Tiwari, V.N. A Novel Method for Accurate Estimation of Hrv from Smartwatch PPG Signals. In Proceedings of the 2017 39th Annual International Conference of the IEEE Engineering in Medicine and Biology Society (EMBC), Jeju, Republic of Korea, 11–15 July 2017; pp. 109–112.
44. Lin, W.-H.; Wu, D.; Li, C.; Zhang, H.; Zhang, Y.-T. Comparison of Heart Rate Variability from PPG with That from ECG. In Proceedings of the International Conference on Health Informatics: ICHI 2013, Vilamoura, Portugal, 7–9 November 2013; Springer: Berlin/Heidelberg, Germany, 2014; pp. 213–215.
45. Liu, W.; Fang, X.; Chen, Q.; Li, Y.; Li, T. Reliability analysis of an integrated device of ECG, PPG and pressure pulse wave for cardiovascular disease. *Microelectron. Reliab.* **2018**, *87*, 183–187. [CrossRef]
46. Charlton, P.H.; Celka, P.; Farukh, B.; Chowienczyk, P.; Alastruey, J. Assessing mental stress from the photoplethysmogram: A numerical study. *Physiol. Meas.* **2018**, *39*, 054001. [CrossRef] [PubMed]
47. Allen, J. Photoplethysmography and its application in clinical physiological measurement. *Physiol. Meas.* **2007**, *28*, R1. [CrossRef]
48. Das, S.; Pal, S.; Mitra, M. Real Time Heart Rate Detection from PPG signal in Noisy Environment. In Proceedings of the 2016 International Conference on Intelligent Control Power and Instrumentation (ICICPI), Kolkata, India, 21–23 October 2016; pp. 70–73.
49. Esgalhado, F.; Fernandes, B.; Vassilenko, V.; Batista, A.; Russo, S. The application of deep learning algorithms for ppg signal processing and classification. *Computers* **2021**, *10*, 158. [CrossRef]
50. De Pedro-Carracedo, J.; Fuentes-Jimenez, D.; Ugena, A.M.; Gonzalez-Marcos, A.P. Transcending Conventional Biometry Frontiers: Diffusive Dynamics PPG Biometry. *Sensors* **2021**, *21*, 5661. [CrossRef]
51. Zhu, Q.; Tian, X.; Wong, C.-W.; Wu, M. ECG Reconstruction via PPG: A Pilot Study. In Proceedings of the 2019 IEEE EMBS International Conference on Biomedical & Health Informatics (BHI), Chicago, IL, USA, 19–22 May 2019; pp. 1–4.
52. Eesa, A.S.; Arabo, W.K. A Normalization Methods for Backpropagation: A Comparative Study. *Sci. J. Univ. Zakho* **2017**, *5*, 319–323. [CrossRef]
53. Chakraborty, A.; Sadhukhan, D.; Mitra, M. A Robust PPG Time Plane Feature Extraction Algorithm for Health Monitoring Application. In Proceedings of the 2018 15th IEEE India Council International Conference (INDICON), Coimbatore, India, 16–18 December 2018; pp. 1–6.
54. Turki, E. An Algorithm for Real-Time Morphology-Based Pulse Feature Extraction from Photoplethysmography (PPG) Signals. Ph.D. Thesis, University of California, Santa Barbara, CA, USA, 2020.
55. Gardner, M.; Randhawa, S.; Reynolds, K.J.; Malouf, G. Estimation of Heart Rate During Sleep Measured from a Gyroscope Embedded in a CPAP Mask. In Proceedings of the 2016 IEEE EMBS Conference on Biomedical Engineering and Sciences (IECBES), Kuala Lumpur, Malaysia, 4–8 December 2016; pp. 646–651.
56. Liu, Y.-Y.; Lv, Y.-X.; Xue, H.-B. Intelligent Wearable Wrist Pulse Detection System Based on Piezoelectric Sensor Array. *Sensors* **2023**, *23*, 835. [CrossRef]
57. Duan, J.; Wang, Q.; Zhang, B.; Liu, C.; Li, C.; Wang, L. Accurate detection of atrial fibrillation events with RR intervals from ECG signals. *PLoS ONE* **2022**, *17*, e0271596. [CrossRef]
58. Panda, A.; Pinisetty, S.; Roop, P. A Novel Mapping of ECG and PPG to Ensure the Safety of Health Monitoring Applications. *IEEE Embed. Syst. Lett.* **2022**, *15*, 49–52. [CrossRef]
59. Panda, A.; Pinisetty, S.; Roop, P. Runtime Monitoring and Statistical Approaches for Correlation Analysis of ECG and PPG. *arXiv* **2022**, arXiv:2202.00559.
60. Kuo, T.B.; Yang, C.C. Sexual dimorphism in the complexity of cardiac pacemaker activity. *Am. J. Physiol. Circ. Physiol.* **2002**, *283*, H1695–H1702. [CrossRef] [PubMed]
61. Task Force of the European Society of Cardiology the North American Society of Pacing Electrophysiology. Heart rate variability: Standards of measurement; physiological interpretation; clinical use. *Circulation* **1996**, *93*, 1043–1065. [CrossRef]
62. Madden, K.M.; Levy, W.C.; Stratton, J.R. Aging affects the response of heart rate variability autonomic indices to atropine and isoproteronol. *Clin. Med. Insights Geriatr.* **2008**, *1*, 17–25.
63. Cheng, B.; Liu, G. Emotion Recognition from Surface EMG Signal Using Wavelet Transform and Neural Network. In Proceedings of the 2008 2nd International Conference on Bioinformatics and Biomedical Engineering, Shanghai, China, 16–18 May 2008; pp. 1363–1366.
64. Davidson, R.J.; Sherer, K.R.; Goldsmith, H.H. *Handbook of Affective Sciences*; Oxford University Press: Oxford, UK, 2009.
65. Wong, A.; Figueroa, A.; Sanchez-Gonzalez, M.A.; Son, W.-M.; Chernykh, O.; Park, S.-Y. Effectiveness of tai chi on cardiac autonomic function and symptomatology in women with fibromyalgia: A randomized controlled trial. *J. Aging Phys. Act.* **2018**, *26*, 214–221. [CrossRef]
66. Wei, Z.; Li, M.; Tang, Y. Fingertip Pulse Rate Variability Extraction Based on Extreme-Point Symmetric Mode Decomposition. *J. Phys. Conf. Ser.* **2022**, *2246*, 012085. [CrossRef]
67. Montgomery, D.C.; Peck, E.A.; Vining, G.G. *Introduction to Linear Regression Analysis*; John Wiley & Sons: Hoboken, NJ, USA, 2021.

68. Su, X.; Yan, X.; Tsai, C.L. Linear regression. *Wiley Interdiscip. Rev. Comput. Stat.* **2012**, *4*, 275–294. [CrossRef]
69. Cohen, I.; Huang, Y.; Chen, J.; Benesty, J. Pearson Correlation Coefficient. In *Noise Reduction in Speech Processing*; Springer: Berlin/Heidelberg, Germany, 2009; pp. 1–4.
70. Nelson, L.S. The Anderson-Darling test for normality. *J. Qual. Technol.* **1998**, *30*, 298. [CrossRef]
71. Roach, D.; Wilson, W.; Ritchie, D.; Sheldon, R. Dissection of long-range heart rate variability: Controlled induction of prognostic measures by activity in the laboratory. *J. Am. Coll. Cardiol.* **2004**, *43*, 2271–2277. [CrossRef]
72. Jerath, R.; Edry, J.W.; Barnes, V.A.; Jerath, V. Physiology of long pranayamic breathing: Neural respiratory elements may provide a mechanism that explains how slow deep breathing shifts the autonomic nervous system. *Med. Hypotheses* **2006**, *67*, 566–571. [CrossRef] [PubMed]
73. Grossman, P.; Taylor, E.W. Toward understanding respiratory sinus arrhythmia: Relations to cardiac vagal tone, evolution and biobehavioral functions. *Biol. Psychol.* **2007**, *74*, 263–285. [CrossRef] [PubMed]
74. Pinheiro, C.H.D.J.; Medeiros, R.A.R.; Pinheiro, D.G.M.; Marinho, M.D.J.F. Spontaneous respiratory modulation improves cardiovascular control in essential hypertension. *Arq. Bras. Cardiol.* **2007**, *88*, 651–659. [CrossRef] [PubMed]
75. Graham, J.M.; Janssen, S.A.; Vos, H.; Miedema, H.M. Habitual traffic noise at home reduces cardiac parasympathetic tone during sleep. *Int. J. Psychophysiol.* **2009**, *72*, 179–186. [CrossRef] [PubMed]